L. Vikingsson et al., Int J Artif Organs 2015; 38(12): 659-666. DOI: 10.5301/ijao.5000457

The implantation of a Polycaprolactone scaffold with subchondral bone anchoring ameliorates nodules formation and other tissue alterations

Line Vikingsson[*1], María Sancho-Tello[2], Amparo Ruiz-Saurí[2], Santos Martínez Díaz[3], José A. Gómez-Tejedor[1,4], Gloria Gallego Ferrer[1,4], Carmen Carda[2], Joan C. Monllau[3], José L. Gómez Ribelles[1,4]*

[1]Centre for Biomaterials and Tissue Engineering (CBIT), Universitat Politècnica de València, 46022 Valencia, Spain.
[2]Departamento de Patología, Universitat de València and INCLIVA Hospital Clínico Universitario, 46010 Valencia, Spain.
Hospital del Mar, Universitat Autònoma de Barcelona, 08193 Bellaterra, Spain.
[4]Ciber en Bioingeniería, Biomateriales y Nanomedicina (CIBER-BBN), Spain.
**Corresponding author. Tel: + 963877007, ext. 88939. Fax: +34 963877276. Center for Biomaterials and Tissue Engineering, Universitat Politècnica de València, Camino de vera s/n, 46002 Valencia, Spain. E-mail: linevikingsson@gmail.com*

Int J Artif Organs 2015; 38(12): 659-666

DOI: 10.5301/ijao.5000457

L. Vikingsson et al., Int J Artif Organs 2015; 38(12): 659-666. DOI: 10.5301/ijao.5000457

Abstract

Introduction: Articular cartilage has limited repair capacity. Two different implant devices for articular cartilage regeneration have been tested *in vivo* in a sheep model to evaluate the effect of subchondral bone anchoring for tissue repair.

Methods: The implants have been placed with press-fit technique in a cartilage defect after microfracture surgery in the femoral condyle of the knee joint of the sheep and histologic and mechanical evaluation was done 4.5 months later. The first group consists of a biodegradable Polycaprolactone, PCL, scaffold with double porosity. The second test group consists of a PCL scaffold attached to a Poly(L-lactic acid), PLLA, pin anchored to the subchondral bone.

Results: For both groups most of the defects (75%) exhibited the articular surface completely or almost completely repaired with a neotissue. Nevertheless, the surface had a rougher appearance than controls and the repair tissue was immature. In the trials with solely scaffold implantation, severe subchondral bone alterations were seen with many large nodular formations. These alterations were ameliorated when implanting the scaffold with a subchondral bone anchoring pin.

Discussion: The results show that tissue repair is improved by implanting a PCL scaffold compared to solely microfracture surgery, and most importantly, that subchondral bone alterations, normally seen after microfracture surgery, were partially prevented when implanting the PCL scaffold with a fixation system to the subchondral bone.

Keywords:

Tissue engineering, cartilage engineering, biomaterials, polycaprolactone, subchondral bone alterations

1. Introduction

Articular cartilage has limited repair capacity after damage or loss of tissue. This is mainly due to the avascular nature of the cartilage, which implies that no recruiter cells can arrive to the defect. There exist different surgical treatments that intent to restore the damaged tissue. Not all cartilage defects are treated in the same way, the decision of which surgery or treatment to chose is based on size and nature of the defect, weighted with the patient age, physical condition and recovery expectations. (1) Bone marrow stimulation techniques aim at repairing the articular cartilage with help of bone marrow mesenchymal stem cells, bMSC, recruited from the subchondral bone. The most common bone marrow stimulation technique is microfracture surgery invented by Steadman *et al*. in 1994. (2) Damaged cartilage is totally removed and holes are drilled down to the subchondral bone, making sure not damaging the subchondral plate. These perforations provoke bleeding and release of marrow elements, such as mesenchymal stem cells and growth factors. The defect is soon filled with a fibrin clot. The abraded surface of the subchondral bone is rough and good for clot attachment. It has been reported that pluripotent bone marrow progenitor cells differentiate to chondrocyte-like cells and produce a cartilaginous repair tissue that fills the chondral defect. (3) (4) Microfracture is recommended for young patients with small or medium sized defects, but have shown long-term failure for defects bigger than 3 cm^2. (1) (5) (6) Pridie drilling and abrasion techniques also take advantage of the pluripotency of adult stem cells in subchondral bone marrow. (7) (8) Autologous chondrocyte implantation, ACI, is shown to give a slower recovery process, but similar success ratio in returning to physical activities as the microfracture. Clinical long-term results indicate that ACI give better outcome compared to microfracture in high physical activity patients. (5) Third generation ACI which uses the patients own chondrocytes for cell-culture and re-implantation in combination with a collagen membrane, is shown to be a promising treatment option. (9) (10) For medium size lesions autologous osteochondral transfer could be the best treatment option. The disadvantages of this technique are low donor site availability and the size-limits of the defect. (11) (12)

Tissue Engineering is an interdisciplinary science aiming at restoring damaged tissue or organs with 3-dimensional scaffolds, growth factors and/or cells. (13) (14) The scaffold must sustain initial mechanical load in the tissue and protect cells from excessive forces, i.e. diminish differences in stress-strain response with respect to neighboring tissue. (15) It is at the same time important that the scaffold permits transmitting appropriate mechanical signals to cells to allow mechanotransduction. (16) The amount of glycosaminoglycans, GAGs, produced is directly proportional to the load applied: Static compression of cartilage explants decreases extracellular matrix, ECM, production while dynamic compression increases ECM production. (17) (18) (19) The p(DA, #30)(DA, #30)orosity of the 3-dimensional scaffold is also important for cell-seeding and cell ingrowth, as for transport of nutrients and waste products. (15) (20) (21) (14) (22)

Most scaffold implants suffer from long-term failure or have similar results as conventional surgical treatments. A successful cartilage implant will improve tissue regeneration and most importantly, improve patient life quality after operation. The perfect implant should also be user-friendly, reduce operation time and number of surgical interventions in order to save operative steps and costs. All these factors must be taken into account when designing, fabricating and manufacturing scaffolds for pre-clinical and clinical trials.

Some implants focus on press-fit technique with biodegradable subchondral bone fixation systems, but perforate the subchondral bone to a high extend. (23) It is shown that by perforation of the subchondral bone plate, as in microfracture and in higher extent osteochondral implants, the subchondral bone suffer alterations such as cyst formation, intralesional osteophytes, thickening of the subchondral bone and thinning of the articular cartilage surface. (11) (24) (23) (25) (26) (27) The awareness of subchondral bone pathology after surgical interventions is recently increasing. It can be seen that alterations of subchondral bone have important consequences for the healing process of the whole joint over time. Clinical studies have seen subchondral bone alterations in 30% of patients treated with microfracture.(24) (26)

Therefore, this study evaluates the effect of subchondral bone anchoring on tissue regeneration. The study has tested a cartilage implant based on a European patented biomedical device, with patent number EP201131625 PCT/WO2013/178852. The implant consists of a porous sponge and a biodegradable subchondral bone anchoring system, based on a thin pin. One test group had a chondral scaffold implanted after microfracture, and the second test group was implanted with the same scaffold attached to a biodegradable pin anchored to the subchondral bone. The results were tested against controls with only microfracture surgery. The advantage and novelty of our device compared to others commercially available implants (23) is that the bone anchoring system is very thin, causing minimal damage to the subchondral bone during the implantation. Our study demonstrates significant improvements in the tissue repair of the articular cartilage compared to microfracture surgery, and improved tissue repair with subchondal bone anchoring than without the subchondral bone fixation system.

2. Methods

2.1. Scaffold fabrication

A Polycaprolactone scaffold was synthesized by freeze extraction and porogen leaching method as previously described in other works.(20) (28) (29) (30) (31) Briefly: A 15% PCL solution (average molecular weight 80000 Da, Mw/Mn <2, Sigma Aldrich, Spain) in 1.4 dioxane (Sigma Aldrich, Spain) was prepared and mixed rapidly with 1:1.25 weight ratio PCL solution/porogen microspheres. Microspheres of Elvacite 2043, a mixture of low molecular weight Poly(Ethyl Methacrylate), PEMA, and Poly(Methyl Methacrylate), PMMA, with diameters ranging from 120 to 200 µm were purchased from Lucite International (USA). The mixture was rapidly frozen in liquid nitrogen. Cold, -20° C, ethanol (99%

pure Scharlab, Spain) was poured on top of the polymers. Dioxane was extracted during three days with daily changes of cold ethanol, creating micro-porosity in the remaining scaffold. The porogen microspheres were then leached out in 40° C ethanol during eight days, or until no traces of microspheres were found in the solvent. Scaffolds were cut with circular stamps and surgical scalpels to cylinders of 4 mm diameter and 1 mm height. For the second trial group, the PCL scaffold was fixed to the subchondral bone using a PLLA pin (Contour™ Meniscus Arrow™, ConMed, USA) as shown in Figure 1.

Figure 1. The implant device employed in the second trial group, consisting of a porous PCL scaffold attached to a PLLA pin. Scale bar 4 mm.

The PCL scaffold was synthesized from a 25% PCL solution and 1:1 PCL solvent/porogen spheres ratio to increase the mechanical properties of the scaffold. The head of the PLLA arrow was melted to 200 °C (IN2100 Quick Soldering Iron, JBC, Spain) to have a flat end. The arrow was attached to the PCL solution before freezing the mixture PCL solution/porogen in liquid nitrogen. The rest of the synthesizing steps were performed as for the scaffolds without anchoring pin. Once obtained, the scaffolds were dried in vacuum until constant weight, and placed individually in Eppendorf tubes and sealed in

vacuum pockets. The material was sent to sterilization with gamma rays with a dose of 25 kGys (Aragogamma, Spain).

2.2. Animals implantation

Sixteen mature female sheep, breed Merina and official brand 270BK (Supplier Agricola Ramadera Les Anglades Vilert, Girona, Spain), were employed. The surgical interventions were carried out at the Hospital Clínic Veterinari at the Universitat Autònoma de Barcelona, UAB. The animals were taken care by the Departament de Medicina i Cirugia Animals at UAB before, under and after surgery. The sheep weighed about 40 kg. The trials were realized in accordance to protocol CEEA 1940 17-02-2013 approved by the Ethic Committee for animal trials at the UAB. The protocol follows the European regulations 86/609/EEC (European Economic Community) and law 5/1995 with decision 1201/2005 from the local government. After surgery the animals spent a postoperative period in boxes and were released after seven days in conventional herd at UAB, named “Servei de Granges I Camps Experimentals” number B9900042. The animals were divided into three groups: 7 animals underwent microfracture surgery with PCL scaffold implantation, 6 animals underwent microfracture surgery with PCL scaffold and PLLA arrow implantation and 3 animals underwent only microfracture surgery (see the details of these experiments in Table 1).

	Group 1 PCL scaffold	**Group 2** PCL scaffold +PLLA pin	**Group 3** microfracture
Number of animals	7	6	3
Number of nodules/animal	2.29 ± 0.61	2.83 ± 1.49	2.33 ± 0.88
Area (mm^2)/nodule	0.96 ± 0.40	1.23 ± 0.39	1.71 ± 0.76
Total area (mm^2)/animal	2.97 ± 1.20	2.63 ± 0.78	5.33 ± 3.64
Distance (mm)	1.25 ± 0.35	1.91 ± 0.50	1.40 ± 0.37

Table 1. Morphometric data of the nodular formations observed within subchondral bone. Values express mean value ± standard error for each group. No statistically significant differences were observed by one-way ANOVA in any of the parameters studied.

The sheep were anesthetized by tracheal intubation and laid in supine position. Sterile field was prepared following standard procedures: First the right knee was shaved and the surgical site was disinfected using iodine solution, and animal non-sterile zone was covered with sterile towels. A 40 mm incision was performed in the medial knee in distal position to patella. An internal distal arthrotomy was performed in the lower part of the patella in the medial height of patellar tendon, separating sidelong the patellar ligament and the patella, without dislocating the joint, and separating the internal structures of the joint capsule allowing access to the load bearing zone of the internal condyle of femur.

The first experimental group with 7 animals underwent surgery with 2 chondral lesions of 4 mm diameter in the weight-bearing zone of the internal femoral condyle, with 4-5 microfractures until bleeding from subchondral bone. To

perform the microfractures, an Arthrex awl used in human microfracture surgery was employed. The defect was washed with physiologic serum. The PCL scaffold was implanted by press-fit technique. The second group of 6 animals underwent the same surgery, with the addition of an orifice in the middle of the chondral lesion performed by a Kirschner needle. The orifice was made to facilitate the implantation of the PCL scaffold with PLLA pin. The implant was put in place with press-fit technique. The third group, with 3 animals, underwent the same surgery as first group, with 2 chondral lesions and 4-5 microfractures, but without any posterior scaffold implantation. In all groups the arthrotomy was closed with loose vycril sutures 3/0, and the skin with continuous vycril sutures 4/0 and loose paper (Steri-Strip 3M) sutures. The lesion was covered with standard bandage (Sterile Cutiplast 7.2 cm x 5 cm, Smith&Nephew). After surgery and removal of anesthesia the animals were returned to cages, wearing soft knee bandage in flexion position for 7 days. The animals were standing up about half an hour after operation. After 7 days the animals were released in controlled herds according to the norms approved by CEEA.

The sheep were sacrificed after 4.5 months of free movement in the herd. The animals were first placed in boxes and euthanized by intravenous overdose of pentobarbital 100 mg/kg. Once euthanized the samples were obtained by dissection of the right knee and exposure of the internal femoral condyle, by osteotomy with an oscillating saw. The internal femoral condyle of the left knee was also obtained, to use as native control.

2.3. Histological and morphometric analysis

Articular surface was macroscopically studied, and pictures of the femoral condyles were taken using a Leica DC150 camera. Then, microscopic morphology was studied following standard histological technique. Briefly, after fixing the joint specimen with 4% formaldehyde buffered solution (VWR Chemicals) for 48 hours at room temperature, the samples were rinsed with PBS and immersed in Osteosoft decalcifier solution (Merck) up to 4 months at room temperature. Once the specimens were decalcified, they were cut through the middle of the scaffold and each half was separately embedded in paraffin. Sections of 5-μm thickness were obtained and stained with Hematoxylin-Eosin, HE, and Masson's trichrome staining. The samples were analyzed under an optical microscope (Leica DM 4000B), and histological pictures were taken (Leica DFC 420). The samples obtained in the second trial followed the same procedure except they were embedded in low-melting polyester wax (VWR International) instead of standard paraffin, in order to preserve the implanted biomaterial.

Morphometric software (Image proPlus 7.0) was used to objectively quantify nodules appeared within subchondral bone. The parameters studied were: number of nodules per sample, area of each nodule (mm^2/nodule), total area of the nodules per sample (mm^2/sample), and minimum distance (mm) from each nodule to the articular surface.
Database of Image proPlus software was exported to Microsoft office Excel (Version 2010), and variables were statistically analyzed using of IBM SPSS

Statistics for Windows, Version 19.0. (Armonk, NY: IBM Corp.). Data are expressed as mean values ± SE.
After applying the Shapiro-Wilk normality test, we found that we cannot reject the null hypothesis in any of the variables; therefore they follow a normal distribution. Once equality of variances was assumed, we carried out an analysis of variance (ANOVA) to compare all the variables. Statistically significant differences were set at the $p < 0.05$ level.

2.4. Mechanical testing

Indentation tests were performed at the cartilage explants from the first trial group. The samples were sent in sterile PBS buffer medium with penicillin/streptomycin 1ml/100 ml PBS with 0.5% azide (>99.5%, ReagentPlus®, Sigma-Aldrich, Spain) and controlled temperature (4° C). After indentation tests the samples were fixed in formalin solution 10% neutral buffer (Sigma-Aldrich, Spain) for 48 hours. Then the samples were washed and saved in PBS+azide and sent to histological examination. For the indentation test the specimen was cut with an oscillating saw to smaller pieces to fit in the experimental instrument. The whole cartilage piece with the subchondral bone was subjected and indentation was performed by a cylindrical rod of 1.025 mm diameter with a flat surface in a Thermo-Mechanical Assay machine, TMA (Seiko TMA/SS6000, Japan). A compression program with loading to 125 g with 10 g/min under water-immersed conditions and 38° C was carried out. In the stress-strain graph plotted from the obtained data the first strains are neglected, until a positive force. Poisson´s coefficient is estimated to 0.4 and the thickness of the cartilage is estimated from posterior histology pictures.(32) (31)

3. Results

Figure 1 shows the PCL scaffold with PLLA subchondral bone anchoring, used in the second trial group. The implant used in the first trial group consists of solely the PCL chondral part, without any anchoring system. The mechanical properties of half of the animals in the first test group were evaluated by indentation test. As seen in table 2 the repair tissue had inferior mechanical properties than healthy native hyaline cartilage. This is believed to be due to the relatively immature repair tissue seen in the defects, due to the relatively short (4.5 months) implantation time.

	Elastic Modulus (MPa)	
Sample	Control	Scaffold
1	0.62 ± 0.04	0.34 ± 0.08
2	0.42 ± 0.10	0.06 ± 0.02
3	0.59 ± 0.14	0.17 ± 0.15

Table 2. The elastic modulus of the explants from the first trial group, with PCL scaffold. Values are expressed as mean ± SD. The controls are tested from the healthy contralateral joint in the same animals (N=3).

Macroscopic study of the articular surface at the injury zones shows the appearance of neotissue covering partially or completely the injury zone, although the surface had a rougher appearance than controls. No differences were found in the macroscopic study of the articular surface in the different groups of treatment. However, when samples were sectioned into halves, big nodular formations were observed in the subchondral bone of 71.4% of the samples (5 of 7) of the first group, as it was confirmed microscopically (Figures 2 and 3), similarly to those observed in other studies using large mammals (33). In this group, 2.29±0.61 nodules were observed in each animal, with a mean area of 0.96±0.40 mm^2 per nodule, a total area of 2.97±1.20 mm^2 occupied by nodules in each animal, and a mean distance of 1.25±0.35 mm from the nodules to articular surface (Table 1).

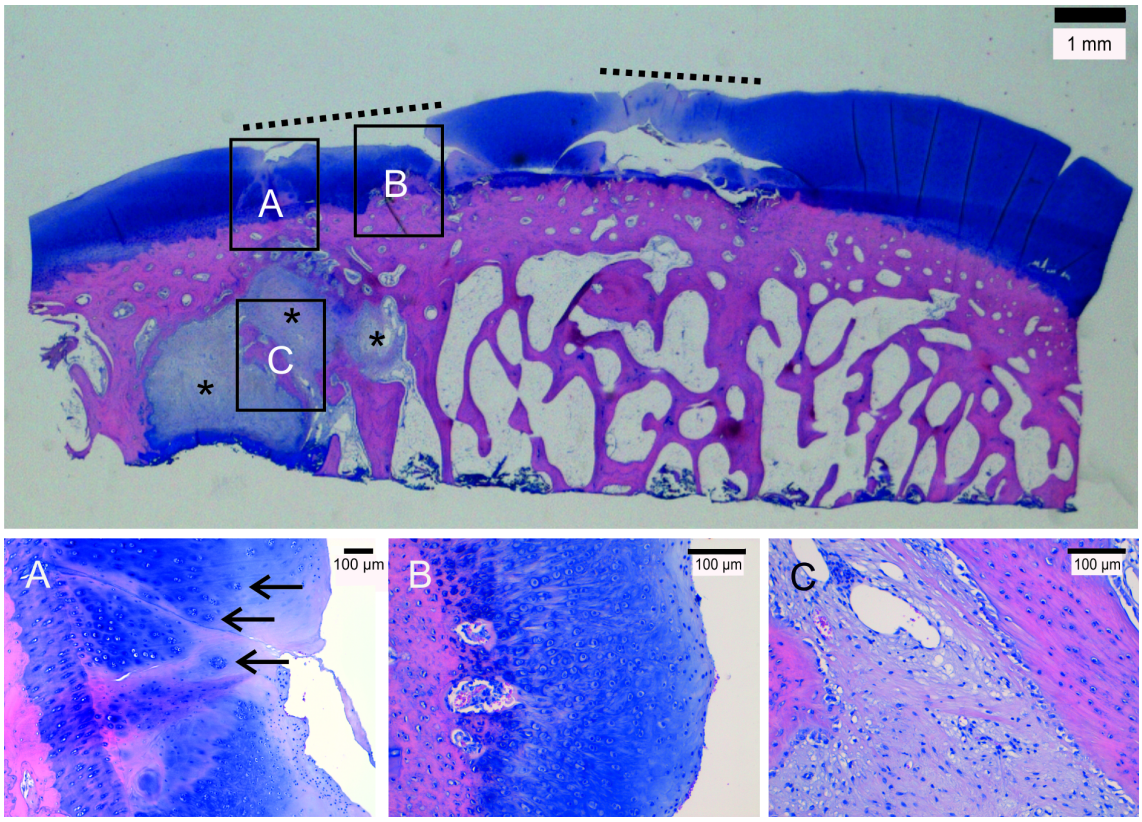

Figure 2. Panoramic view of a sample 4.5 month after implantation of only PCL scaffold and microfracture surgery. The two defects (dashed lines) are seen partially filled with a neotissue and the subchondral bone is showing alterations with large nodular formation (asterisks). Scale bar 1mm. a) Limit between native cartilage and neotissue, with many isogenic groups containing abundant cells (arrows), b) neocartilage growth at the defect site, and c) small cyst within a regenerative nodule in the subchondral bone. Scale bar 100 µm.

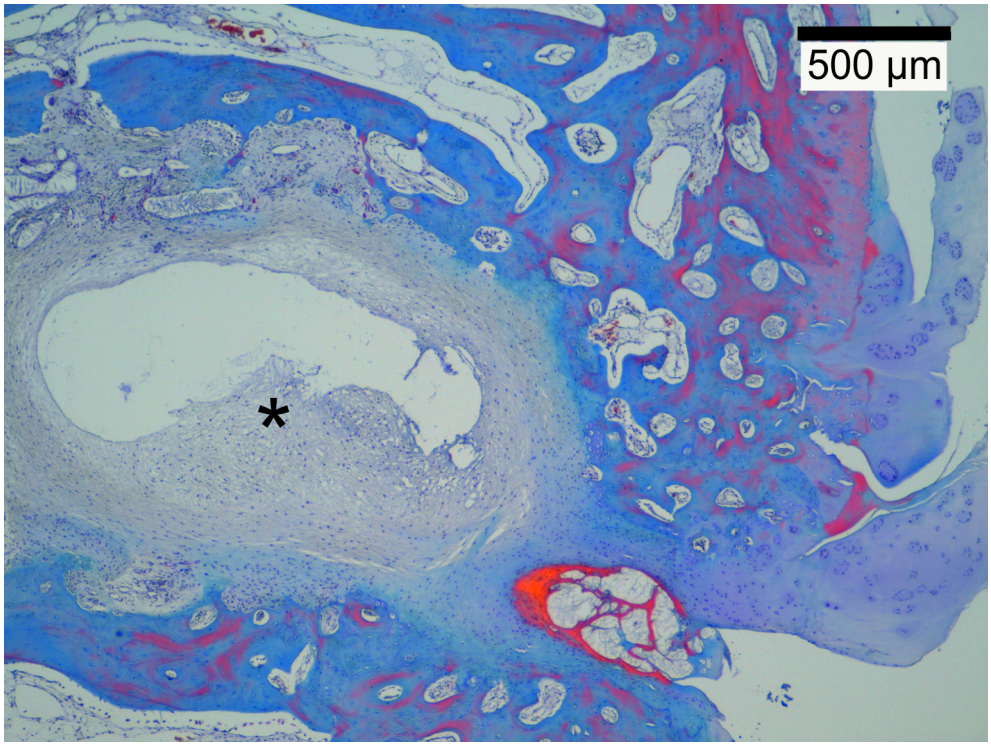

Figure 3. Microscopic image of sample 4.5 months after implantation of only PCL scaffold. A regenerative nodule is observed (asterisk), containing areas of immature or loose connective tissue and a central cystic cavity. Scale bar 500 µm.

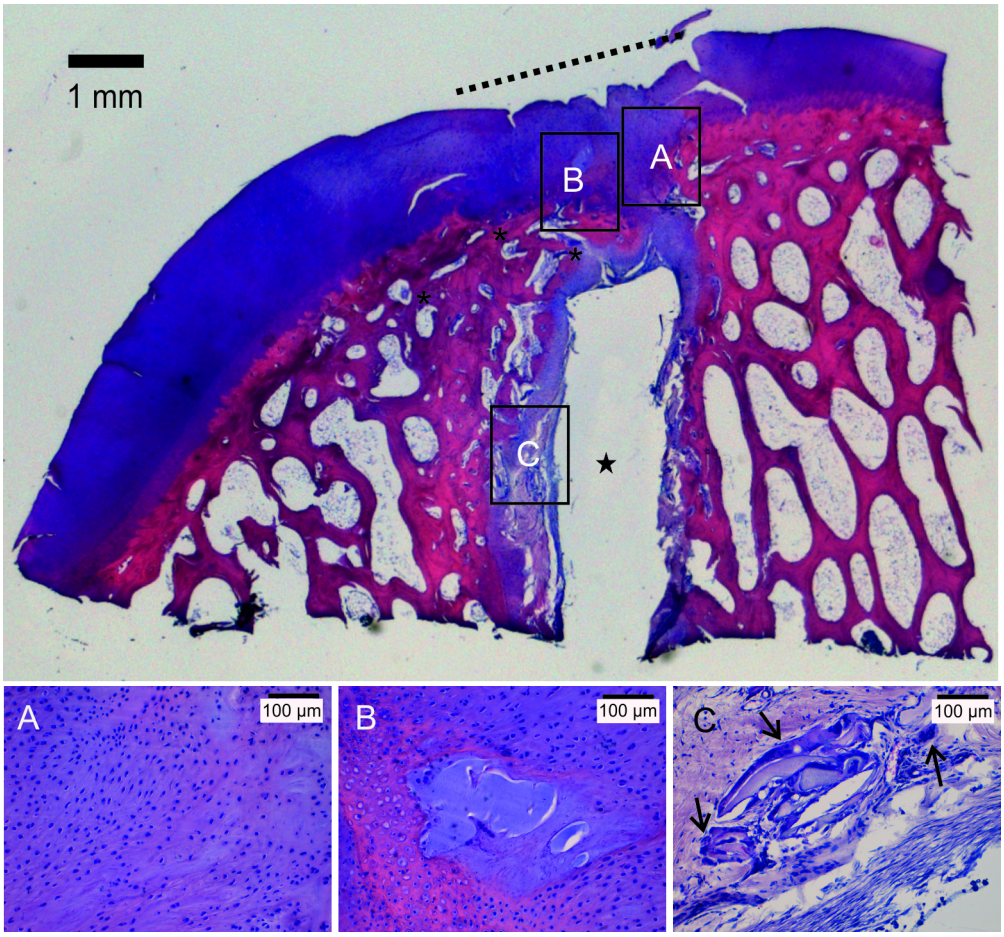

Figure 4. Panoramic view of a sample after 4.5 months implantation of PCL scaffold with subchondral bone anchoring pin. The defect (dashed line) is filled with a neotissue, and subchondral bone lacks any alteration. The white area (star) represents the space occupied by the anchoring pin. Scale bar 1mm. a) Regenerated neotissue is immature cartilaginous tissue, b) remains of PCL scaffold, degraded or broken into smaller pieces, surrounded by regenerated neotissue, and c) remains of PLLA pin degraded by multinucleated phagocitic cells (arrows). Scale bar 0.1 µm.

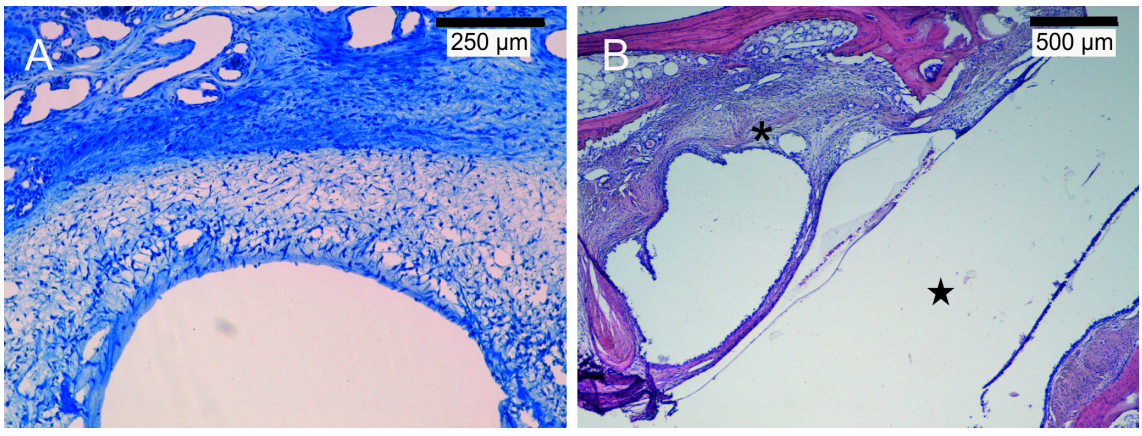

Figure 5. Microscopic image of a sample 4.5 months after implantation of PCL scaffold with subchondral bone anchoring pin. a) Tissue surrounding the anchoring pin, composed by an inner layer of mesencymal or loose connective tissue and an outer layer of fibrous connective tissue. Scale bar 250 µm. b) A small nodule (asterisk) with a cystic cavity observed at the deepest end of the anchoring pin (star). Scale bar 500 µm.

The presence of nodules in the second group was similar to the first one (83.3%, 5 of 6 samples), they occupied a smaller total area (2.63±0.78 mm^2) and were located deeper (1.91±0.50 mm) than those of the first group (Figure 5, although no statistically significant differences were observed (Table 1).

Microscopic study of the articular surface revealed that all samples presented an active process of neotissue formation around the edges of the injury, as previously published in smaller mammals (34). In some samples, neotissue covered completely the articular surface (although the thickness was less than non-treated surface) but in others the neotissue only covered partially the implanted scaffold, which was then in contact to sinovial cavity, in both trials studied. Figures 2 and 4 represent typical results from both groups.

In the first group (only PCL scaffold), the repaired tissue on articular surface showed the appearance of hyaline-like cartilage in some places (Figure 2b), whereas fibrous cartilage or fibrous connective tissue was observed in other areas. Microscopic analysis revealed that the native cartilage at the edges of the cavity showed active proliferation, since isogenous groups contained abundant cells within a single lacuna (Figure 2a). The neotissue formed filling the cavity at the articular surface was mainly immature hyaline cartilage, with a higher cellular density than native cartilage (thus, with less extracellular matrix produced), whose cells did not present the arrangement of mature hyaline cartilage (Figure 2 a-b). Subchondral bone nodules were big and abundant in the first trial, and they contained some empty areas (cystic cavities) or immature connective tissue (Figures 2c and 3), and they resembled regenerative areas. In addition, samples with the same surgery procedure but without any scaffold implanted (third group, Figure 6) also showed similar nodular formations in the subchondral bone in all samples studied (3 of 3), but neotissue grown on the surface showed thin areas with hyaline-like cartilage aspect in some areas along with vascularized fibrous connective tissue in others.

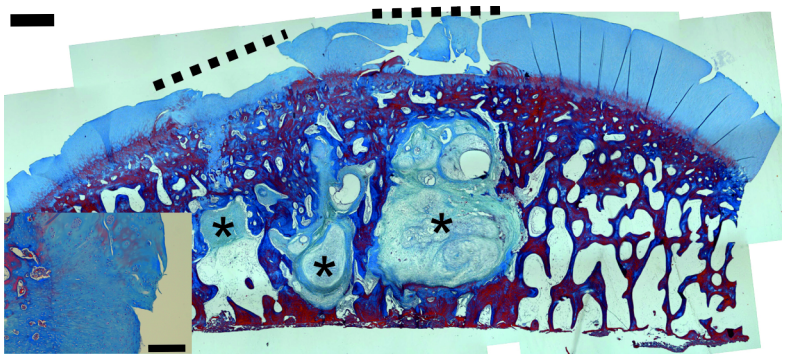

Figure 6. Microscopic image of a sample 4.5 months after microfracture surgery with no scaffold implanted in the defects (dashed lines). The regenerated tissue on surface (inset) presents areas of hyaline-like cartilage aspect along with other with vascularized fibrous connective

tissue. Big regenerative nodules (asterisks) are seen within the subchondral bone. Scale bar 1 mm panoramic image and inset 250 µm.

In the second group, where the PCL scaffold was attached to a PLLA anchoring pin, microscopic study revealed an active tissue repair process in the injured surface as well as around the pin (Figure 4). Similar to first trial group, the neotissue found on the articular surface was mainly immature hyaline-like cartilage (Figure 4a), with scarce extracelular matrix between cells in comparison to controls, that did not present an ordered mature pattern. In this case, areas of preserved PCL scaffold could be observed (Figure 4b). In the subchondral bone, the area occupied by the PLLA anchoring pin appeared as an empty rectangular cavity (Figure 4), since this material was lost in the histological process, and it was surrounded mainly by fibrous connective tissue containing big multinucleated cells with a phagocityc aspect (Figure 4c), whereas other surrounding areas also contained loose or mesenchymal connective tissue around the pin cavity and eventually primary bone. In this group, nodules occupied a less extensive total area and were located at a deeper position than other groups, as previously indicated (Figure 5b, Table 1). It seems like the implant with subchondral bone anchoring system improves tissue repair and foremost, diminishes bone alterations. Subchondral bone alterations are normally seen as consequences of microfracture surgery or osteochondral implants, which suggest that the presence of the anchoring pin ameliorates subchondral bone fragility. Both chondral PCL scaffold and PCL/PLLA implant device show improved tissue repair in comparison to microfracture surgery (group 3, Table 1), although no statistically significant differences were found, $p \geq 0.05$. However, the most impact result is seen in the subchondral bone since the fixation system drastically diminishes alterations.

4. Discussion

Regarding the implant consisting of PCL scaffold with subchondral bone anchoring, the macroscopic study showed that most of the cartilage defects were completely or almost completely filled with a neotissue. Nevertheless, they had a rougher appearance than controls. Besides, a less extensive subchondral area was occupied by nodules, which were located deeper than those of the first group. These results showed an improvement from the defects where only PCL scaffold was implanted without anchoring pin at the time studied. Histological study reveals an active repair process in the injured surface as well as around the pin. All samples presented neocartilage formation at the edges of the injury that eventually covered the whole surface in some cases, although the cartilage observed had an immature aspect at the time of study (4.5 months after surgery). Fibrous cartilage or connective tissue was also observed in some areas. Around the pin, fibrous, loose or mesenchymal connective tissues were observed along with an active process of primary ossification, and it presents a reduced area occupied by nodular formations. Therefore, the device implanted improves tissue regeneration in large mammals.

L. Vikingsson et al., Int J Artif Organs 2015; 38(12): 659-666. DOI: 10.5301/ijao.5000457

Acknowledgements

The authors declare no conflict of interest. The authors would like to acknowledge Lara Milián for the histological technique. This work was funded by the Spanish Ministry of Economy and Competitiveness (MINECO) through the project MAT2013-46467-C4-R (including the FEDER financial support). CIBER-BBN is an initiative funded by the VI National R&D&i Plan 2008–2011, Iniciativa Ingenio 2010, Consolider Program. CIBER actions are financed by the Instituto de Salud Carlos III with assistance from the European Regional Development Fund.

References

1. Brittberg M. Which lesions should be treated and why? In: Brittberg M, Gobbi A, Imhoff A, Kon E, Madry H, editors. Cartilage repair: Clinical guidelines-Decision making in cartilage repair-Variable influencing the choice of treatment. First edit. DJO Publications; 2012. p. 3–14.

2. Steadman JR, Rodkey WG, Briggs KK, Rodrigo JJ. The microfracture technique to treat full thickness articular cartilage defects of the knee. Orthopade. 1999;28(1):26–32.

3. Steadman JR, Rodkey WG, Rodrigo JJ. “Microfracture”: surgical technique and rehabilitation to treat chondral defects. Clin Orthop Relat Res. 2001;391:362–9.

4. Steadman JR, Briggs KK, Rodrigo JJ, Kocher MS, Gill TJ, Rodkey WG. Outcomes of microfracture for traumatic chondral defects of the knee: average 11-year follow-up. Arthroscopy. 2003;19(5):477–84.

5. Kon E, Filardo G, Berruto M, Benazzo F, Zanon G, Della Villa S, et al. Articular cartilage treatment in high-level male soccer players: a prospective comparative study of arthroscopic second-generation autologous chondrocyte implantation versus microfracture. Am J Sports Med. 2011;39(12):2549–57.

6. Basad E, Ishaque B, Bachmann G, Sturz H, Steinmeyer J. Matrix-induced autologous chondrocyte implantation versus microfracture in the treatment of cartilage defects of the knee: a 2-year randomised study. Knee Surg Sports Traumatol Arthrosc. 2010;18(4):519–27.

7. Pridie KH. A method of resurfacing osteoarthritic knee joints. J Bone Jt Surg Br. 1959;41:618–9.

8. Insall J. The Pridie debridement operation for osteoarthritis of the knee. Clin Orthop Relat Res. 1974;(101):61–7.

9. Steinwachs M, Waibl B. Autologous matrix associated chondroneogenesis and matrix associated chondrocyte implantation. In: Brittberg M, Gobbi A, Imhoff AB, Kon E, Madry H, editors. Cartilage repair: Clinical guidelines-Decision making in cartilage repair-Variable influencing the choice of treatment. First edit. DJO Publications; 2012. p. 57–70.

10. Brittberg M. Autologous chondrocyte implantation. In: Brittberg M, Gobbi A, Imhoff AB, Kon E, Madry H, editors. Cartilage repair: Clinical guidelines-Decision making in cartilage repair-Variable influencing the choice of treatment. First edit. DJO Publications; 2012. p. 49–56.

11. Quarch VMA, Enderle E, Lotz J, Frosch K. Fate of large donor site defects in osteochondral transfer procedures in the knee joint with and without TruFit plugs. Arch Orthop Trauma Surg. 2014;134(5):657–66.

12. Duda GN, Maldonado ZM, Klein P, Heller MOW, Burns J, Bail H. On the influence of mechanical conditions in osteochondral defect healing. J Biomech. 2005;38:843–51.

13. Langer R, Vacanti JP. Tissue engineering. Science. 1993;260(5110):920–6.

14. Hutmacher DW. Scaffold design and fabrication technologies for engineering tissues - state of the art and future perspectives. J Biomater Sci-Polym Ed. 2001;12(1):107–24.

15. Hutmacher DW. Scaffolds in tissue engineering bone and cartilage. Biomaterials. 2000;21(24):2529–43.

16. Chiquet M, Renedo AS, Huber F, Flück M. How do fibroblasts translate mechanical signals into changes in extracellular matrix production? Matrix Biol. 2003;22(1):73–80.

17. Bryant S, Chowdhury T, Lee D, Bader D, Anseth K. Crosslinking density influences chondrocyte metabolism in dynamically loaded photocrosslinked poly(ethylene glycol) hydrogels. Ann Biomed Eng . 2004;32:407-17.

18. Wang Y, de Isla N, Huselstein C, Wang B, Netter P, Stoltz J, et al. Effect of alginate culture and mechanical stimulation on cartilaginous matrix synthesis of rat dedifferentiated chondrocytes. Biomed Mater Eng. 2008;18:47–54.

19. Appelman T, Mizrahi J, Elisseeff J, Seliktar D. The influence of biological motifs and dynamic mechanical stimulation in hydrogel scaffold systems on the phenotype of chondrocytes. Biomaterials. 2011;32:1508–16.

20. Lebourg M, Suay Antón J, Gómez Ribelles JL. Porous membranes of PLLA–PCL blend for tissue engineering applications. Eur Polym J. 2008;44(7):2207–18.

21. Hollister SJ. Porous scaffold design for tissue engineering. Nat Mater. 2005;4(7):518–24.

22. Buschmann MD, Kim YJ, Wong M, Frank E, Hunziker EB, Grodzinsky AJ. Stimulation of aggrecan synthesis in cartilage explants by cyclic loading is localized to regions of high interstitial fluid flow. Arch Biochem Biophys.; 1999;366(1):1–7.

23. Eduardo P, Batista J, Millan-billi A, Patthauer L, Vera S, Gomez-masdeu M, et al. Magnetic resonance evaluation of TruFit ® plugs for the treatment of osteochondral lesions of the knee shows the poor characteristics of the repair tissue.Knee.; 2014;21(4):827–32.

24. Gomoll AH, Madry H, Knutsen G, van Dijk N, Seil R, Brittberg M, et al. The subchondral bone in articular cartilage repair: current problems in the surgical management. Knee Surgery, Sport Traumatol Arthrosc.; 2010;18(4):434–47.

25. Kon E, Filardo G, Perdisa F, Venieri G, Marcacci M. Clinical results of multilayered biomaterials for osteochondral regeneration. J Exp Orthop. 2014;1(1):10.

26. Orth P, Cucchiarini M, Kohn D, Madry H. Alterations of the subchondral bone in osteochondral repair--translational data and clinical evidence. Eur Cell Mater. 2013;25:299–316.

27. Kreuz PC, Steinwachs MR, Erggelet C, Krause SJ, Konrad G, Uhl M, et al. Results after microfracture of full-thickness chondral defects in different compartments in the knee. Osteoarthr Cartil. 2006;14(11):1119–25.

28. Vikingsson L, Claessens B, Gómez-Tejedor JA, Ferrer GG, Gómez Ribelles JL. Relationship between micro-porosity, water permeability and mechanical behavior in scaffolds for cartilage engineering. J Mech Behav Biomed Mater. 2015;48:60–9.

29. Vikingsson L, Gomez-Tejedor JA, Gallego Ferrer G, Gomez Ribelles JL. An experimental fatigue study of a porous scaffold for the regeneration of articular cartilage. J Biomech. 2015;48(7):1310-7

30. Vikingsson L, Gallego Ferrer G, Gómez-Tejedor JA, Gómez Ribelles JL. An in vitro experimental model to predict the mechanical behaviour of macroporous scaffolds implanted in articular cartilage. J Mech Behav Biomed Mater. 2014;32:125–31.

31. Martinez-Diaz S, Garcia-Giralt N, Lebourg M, Gómez-Tejedor J-A, Vila G, Caceres E, et al. In vivo evaluation of 3-dimensional polycaprolactone scaffolds for cartilage repair in rabbits. Am J Sport Med. 2010;38(3):509–19.

32. Mow VC, Holmes MH, Lai M. Fluid transport and mechanical properties of articular cartilage. J Biomech. 1984;17(5):377–94.

33. Granero-Moltó, F Escribano R, Deplaine H, Ripalda-Cemborain P, Muinos-López E, Gómez-Ribelles JL, Gallego Ferrer G, et al. Articular

Cartilage Regeneration Triggered by Mesenchymal Stem Cells. J Tissue Eng Regen Med. 2015;

34. Sancho-Tello M, Forriol F, Gastaldi P, Ruiz-Saurí A, Martín de Llano J, Novella-Maestre E, et al. Time evolution of “in vivo” articular cartilage repair induced by bone marrow stimulation and scaffold implantation in rabbits. Int J Artif Organs. 2015;38(4):210–23.